ISSN 0021-3640, JETP Letters, 2017, Vol. 105, No. 11, pp. 691–695. © Pleiades Publishing, Inc., 2017.
Published in Russian in Pis'ma v Zhurnal Eksperimental'noi i Teoreticheskoi Fiziki, 2017, Vol. 105, No. 11, pp. 659–663.

FIELDS, PARTICLES, AND NUCLEI

Colormagnetic Confinement in the Quark–Gluon Thermodynamics[1]

M. S. Lukashov[a, b, *] and Yu. A. Simonov[a, **]

[a] Alikhanov Institute for Theoretical and Experimental Physics, Moscow, 117218 Russia
[b] Moscow Institute of Physics and Technology (State University), Dolgoprudnyi, Moscow region, 141700 Russia
*e-mail: lukashov@phystech.edu
**e-mail: simonov@itep.ru

Received April 10, 2017

Nonperturbative effects in the quark–gluon thermodynamics are studied in the framework of vacuum correlator method. It is shown, that for $T > T_0 = 175$ MeV two correlators: colorelectric $D_1^E(x)$ and colormagnetic $D^H(x)$, provide the Polyakov line and the colormagnetic confinement in the spatial planes respectively. As a result, both effects produce the realistic behavior of $p(T)$ and $I(T)$, being in good agreement with numerical lattice data.

DOI: 10.1134/S0021364017110017

1. INTRODUCTION

The idea of a new phase of the QCD matter above some critical temperature has appeared soon after the discovery of QCD, namely in [1–3] were formulated the first principles of weak interacting quark–gluon medium, named the quark–gluon plasma (QGP).

The first lattice studies [4–6] have supported this idea, and it was soon realized that high-energy ion collisions can be used to create QGP, see [7] for a recent review and references.

The subsequent lattice studies of QGP and thermal transitions has discovered a variety of sudden and complicated features of the QGP behavior, especially near the transition temperature T_c [8]. At present, the high accuracy lattice data are obtained for $n_f = 2+1$ QCD in the wide temperature region [9–11].

An important progress was made at large T in the framework of the perturbation theory (Hard Thermal Loop (HTL) theory) [12], where terms up to $O(g^6)$ have been taken into account.

However, in the region $150\text{ MeV} < T < 600$ MeV the nonperturbative (np) effects are most important, which can be taken into account in the framework of the Vacuum Correlator Method (VCM), to be used below.

This method was suggested at the end of the 1980s in [13, 14], stating, that the basic origin of the nonperturbative dynamics in QCD at zero or nonzero T is connected with the vacuum gluonic fields, appearing in the form of gluon vacuum correlators. In FCM, the confinement follows from nonzero quadratic correlator $D^E(x-y)$ of colorelectric (CE) fields $E_i^a(x)$, which produce scalar linear confining interaction $V_D^{(\text{lin})}(r)$, while correlators $D^H(x-y)$ of colormagnetic (CM) fields $H_i^a(x)$, are responsible for confinement in spatial surfaces:

$$\begin{gathered}\frac{g^2}{N_c}\langle\langle \mathrm{Tr} E_i(x)\Phi E_j(y)\Phi^\dagger\rangle\rangle \\ = \delta_{ij}\left(D^E(u) + D_1^E(u) + u_4^2\frac{\partial D_1^E}{\partial u^2}\right) + u_iu_j\frac{\partial D_1^E}{\partial u^2}, \\ \frac{g^2}{N_c}\langle\langle \mathrm{Tr} H_i(x)\Phi H_j(y)\Phi^\dagger\rangle\rangle \\ = \delta_{ij}\left(D^H(u) + D_1^H(u) + \mathbf{u}^2\frac{\partial D_1^H}{\partial \mathbf{u}^2}\right) - u_iu_j\frac{\partial D_1^H}{\partial u^2}.\end{gathered} \tag{1}$$

The confining correlators D^E, D^H generate the nonzero values of CE and CM string tensions,

$$\sigma^{E(H)} = \frac{1}{2}\int D^{E(H)}(z)d^2z. \tag{2}$$

The CE correlators D^E and D_1^E produce the scalar confining interaction $V_D(R)$ and the vector-like nonperturbative interaction $V_1(R)$ respectively.

$$\begin{aligned}V_D(R) &= 2c_a\int_0^r (r-\lambda)d\lambda\int_0^\infty d\nu D^E(\lambda,\nu) \\ &= V_D^{(\text{lin})}(r) + V_D^{(\text{sat})}(r),\end{aligned} \tag{3}$$

[1] The article is published in the original.

$$V_1(r) = c_a \int_0^r \lambda d\lambda \int_0^\infty d\nu D_1^E(\lambda, \nu),$$
$$\text{where} \quad c_{\text{fund}} = 1, \quad c_{\text{adj}} = 9/4. \tag{4}$$

At the beginning of nineties a new theory of temperature transition in QCD was suggested in [15, 16], where at the critical temperature T_c the correlator D^E, and hence CE confinement disappears, while the CM vacuum fields survive.

The advanced form of the np theory of the thermalized QCD was given in [17], where the Polyakov lines have been derived from the vector CE potential $V_1(r,T)$, produced by the CE field correlator $D_1^E(x-y)$.

Recently the approach of FCM for QCD at $T > 0$ was reconsidered with the aim to take into account the most important np contributions: vector CE interaction $V_1(r,T)$ at all T and CM confinement at $T \geq T_c$.

It was shown in [18] that the latter phenomenon resolves the old Linde problem, since it produces the effective CM Debye mass and eliminates IR divergence of perturbative theory, however justifying the necessity of summing up the infinite series of diagrams in the order $O(g^6)$.

In [19, 20], the CM confinement was taken into account together with exact treatment of Polyakov lines in the SU(3) theory. The resulting pressure $p(T)$ and trace anomaly $I(T)$ are in good agreement with lattice data [11].

It is a purpose of the present paper to apply the same method, as in [19, 20], to the analysis of the QCD matter with $n_f > 0$ at $T \geq T_0 = 175$ MeV $(T_0 \geq T_c)$, taking into account accurate values of Polyakov lines and the CM confinement.

Below we explain the general formalism in Section 2. In Section 3, the notation of the CM confinement and its dynamics is treated and the resulting for formulas for $p(T)$, $I(T)$ are obtained. In Section 4, the main dynamical input is defined with respect to $V_1(r,T)$ and Polyakov lines $L(T)$. In Section 5, the numerical results are shown and discussed.

2. GENERAL FORMALISM

In this section, we are using thermodynamics of quarks and gluons in the vacuum background fields (VBF), as formulated in [15]. For the gluon contribution, one obtains

$$\langle F_0^{gl}(B)\rangle_B = -T\int_0^\infty \frac{ds}{s}\xi(s) d^4x (Dz)_{xx}^w e^{-K}$$
$$\times \left[\frac{1}{2} tr\langle\tilde{\Phi}_F(x,x)\rangle_B - \langle tr\tilde{\Phi}(x,x)\rangle\right]. \tag{5}$$

Here, B_μ refers to the VBF, $K = \frac{1}{4}\int_0^s d\tau\left(\frac{dz_\mu(\tau)}{d\tau}\right)^2$, $\xi(s)$ is a regularizing factor at $s = 0$, and

$$\tilde{\Phi}_F(x,y) = P_F P \exp\left(2ig\int_0^t \hat{F}(z(\tau))d\tau\right)$$
$$\times \exp\left(ig\int_y^x \tilde{B}_\mu dz_\mu\right). \tag{6}$$

Here, P_F, P are the ordering operators, and $\hat{F}$ is the field strength of the field B_μ, also $\tilde{\Phi}(x,y)$ is obtained from (6) with $\hat{F} = 0$. The winding path measure is

$$(Dz)_{xy}^w = \lim_{N\to\infty}\prod_{m=1}^N \frac{d^4\zeta(m)}{(4\pi\varepsilon)^2}\sum_{n=0,\pm,\ldots}\frac{d^4p}{(2\pi)^4}$$
$$\times \exp\left[ip_\mu\left(\sum_{m=1}^N \zeta(m) - (x-y)_\mu - n\beta\delta_{\mu 4}\right)\right]. \tag{7}$$

As one can see in (5), there enters the adjoint gluon loop $tr\tilde{\Phi}(x,x)$, which will be a major point of our investigation.

Using the relation $P_{gl}V_3 = -\langle F_0(B)\rangle_B$, one can rewrite (5) as

$$P_{gl} = (N_c^2 - 1)\int_0^\infty \frac{ds}{s}\sum_{n\neq 0} G^{(n)}(s),$$
$$G^{(n)}(s) = \int (Dz)_{on}^w e^{-K}\widehat{tr}_a\langle W_\Sigma(C_n)\rangle. \tag{8}$$

Here, W_Σ is the adjoint Wilson loop with the contour C_n, and $\widehat{tr}_a$ is the normalized adjoint trace.

Note, that we have disregarded so far all perturbative contributions except those possible inside the gluon loop.

We now turn to the quark contribution, which according to [17], can be written in a form, similar to (8)

$$P_q = 2N_c\int_0^\infty \frac{ds}{s} e^{-m_q^2 s}$$
$$\times \sum_{n=1}^\infty (-)^{n+1}[S^{(n)}(s) + S^{(-n)}(s)], \tag{9}$$

$$S^{(n)}(s) = \int (Dz)_{on}^w e^{-K}\frac{1}{N_c}\widehat{tr}\langle W_\sigma(C_n)\rangle. \tag{10}$$

At this point it is important to look into the details of the vacuum dynamics at $T \geq T_0$, where the main contribution is given by the correlators D_1^E and D^H. The first is acting in the temporal surfaces $(i4)$, via the interaction $V_1(r,T)$, which can be written, according to [21] as

$$V_1(r,T) = \int_0^\beta d\nu(1-\nu T)\int_0^r \xi d\xi D_1^E(\sqrt{\xi^2+\nu^2}). \quad (11)$$

Separating, as in [19, 20] the constant term $V_1(\infty,T)$, one obtains in (8), (10) a factorization of the space 3d, where D^H is acting, and the temporal direction, which yields [15, 19, 20]:

$$\begin{aligned} G^{(n)}(s) &= \int (Dz_4)^w_{on} e^{-K_4-J_n^E} G_3(s), \\ S^{(n)}(s) &= \int \overline{(Dz_4)}^w_{on} e^{-K_4-J_n^E} S_3(s). \end{aligned} \quad (12)$$

Here, $G_3(s), S_3(s)$ are 3d closed loop Green's functions

$$\begin{aligned} G_3(s) &= \int (D^3z)_{xx} e^{-K_{3d}} \langle \widehat{tr}_a W_3^a \rangle, \\ S_3(s) &= \int (Dz)_{xx} e^{-K_{3d}} \langle \widehat{tr}_f W_3^f \rangle. \end{aligned} \quad (13)$$

As was shown in [21], V_1 enters in J_n^E, which contributes to PL

$$\begin{aligned} J_n^E &= \frac{n\beta}{2}\int_0^{n\beta} d\nu\left(1-\frac{\nu}{n\beta}\right) \\ &\times \int_0^\infty \xi d\xi D_1^E(\sqrt{\xi^2+\nu^2}), \\ L_{\rm adj}^{(n)} &= \exp\left(-\frac{9}{4}J_n^E\right). \end{aligned} \quad (14)$$

One can see in (14), that for $T \lesssim M_{glp} = 1.5$ GeV, (the gluelump mass) and $n < n^* = \frac{M_{glp}}{T}$, $J_n^E \approx nJ_1^E$, and, hence, $L_{\rm adj}^{(n)} \approx (L_{\rm adj})^n$, $L_{\rm adj} \equiv L_{\rm adj}^{(1)}$.

Here, ${M_{glp}}^{-1}$ is the range of D_1^E, as was discussed in [22].

Inserting over (Dz_4) in (12), one obtains $\int (Dz_4)^w_{on} e^{-K_4} = \frac{1}{\sqrt{4\pi s}} e^{-\frac{n^2\beta^2}{4s}}$ and one has the following form for gluon pressure [19]:

$$\begin{aligned} P_{gl} &= \frac{N_c^2-1}{\sqrt{4\pi}}\int_0^\infty \frac{ds}{s^{3/2}} G_3(s) \\ &\times \sum_{n=\pm1,\pm2,..} e^{-\frac{n^2}{4T^2 s}} L_{\rm adj}^{(n)}. \end{aligned} \quad (15)$$

In a similar way, from (9)–(13) one obtains the quark pressure for one quark flavor with the mass m_q:

$$\begin{aligned} P_q &= \frac{4N_c}{\sqrt{4\pi}}\int_0^\infty \frac{ds}{s^{3/2}} e^{-m_q^2 s} S_3(s) \\ &\times \sum_{n=1,2,..} (-)^{n+1} e^{-\frac{n^2}{4T^2 s}} L_f^{(n)}. \end{aligned} \quad (16)$$

In the next section, we analyze the 3d loop CM contributions in $S_3(s)$, $G_3(s)$.

3. COLORMAGNETIC CONFINEMENT CONTRIBUTION TO $S_3(s)$, $G_3(s)$

As one can see in (13), $G_3(s)$ and $S_3(s)$ contain the contribution of the adjoint and fundamental loops respectively, which are subject to the area law, $\langle \widehat{tr}_i W_3 \rangle = \exp(-\sigma_i\,{\rm area}(W))$, $i =$ fund, adj. Kinetic term is in K_{3d} in (13), so both $G_3(s)$ and $S_3(s)$ are proportional to the Green's functions of two color charges, connected by confining string, from one point x on the loop to another (arbitrary) point, e.g., the point u on the same loop.

There are two ways, how the CM confinement can be taken into account, suggested in [19]. Considering the oscillator interaction between the charges, one obtains

$$G_3^{\rm OSC}(s) = \frac{1}{(4\pi)^{3/2}\sqrt{s}} \frac{M_{\rm adj}^2}{{\rm sh}(M_{\rm adj}^2 s)} \quad (17)$$

and $S_3^{\rm OSC}(s)$ is obtained from (17), replacing $M_{\rm adj}$ by M_f. Here, $M_{\rm adj} = 2\sqrt{\sigma_s} = m_D(T)$, where $m_D(T)$ is the Debye mass, calculated in [23] in good agreement with lattice data [24].

A more realistic form obtains, when one replaces the linear interaction $\sigma_s r \to \frac{\sigma_s}{2}\left(\frac{r^2}{\gamma}+\gamma\right)$, varying the parameter γ in the final expressions, imitating in this way linear interaction by an oscillator potential. Following [19, 20], one obtains

$$\begin{aligned} G_3^{\rm lin}(s) &= \frac{1}{(4\pi s)^{3/2}}\left(\frac{M_{\rm adj}^2 s}{{\rm sh}(M_{\rm adj}^2 s)}\right)^{1/2}, \\ S_3^{\rm lin}(s) &= G_3^{\rm lin}(s)\big|_{M_{\rm adj}\to M_f}, \end{aligned} \quad (18)$$

$$M_f = 2.3\sqrt{\sigma_s(T)}, \quad M_{\rm adj} = 1.5M_f = 3.5\sqrt{\sigma_s(T)}, \quad (19)$$

where we have taken into account as in (13), that S_3 obtains from G_3 replacing adjoint loop W_3 by the fundamental one. Finally, substituting these expressions in (15), (16), one obtains the equations for $P_{gl}^{\rm lin}$, $P_q^{\rm lin}$,

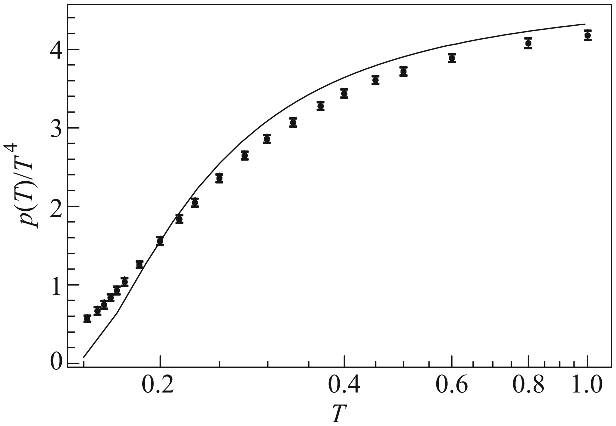

Fig. 1. (Solid line) Plot of $\frac{p(T)}{T^4}$ obtained from Eqs. (15) and (16) in comparison with (points) lattice data from the Budapest–Wuppertal group [11].

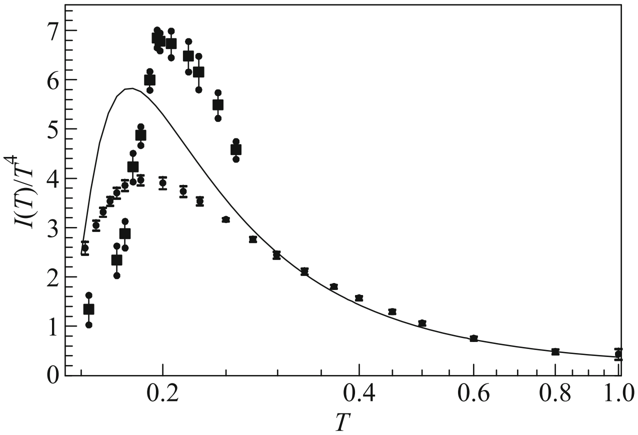

Fig. 2. (Solid line) $\frac{I(T)}{T^4}$ for the pressure given in Fig. 1, (circles) the lattice data from the Budapest–Wuppertal group [11], and (squares) the lattice data from Hot-QCD group [27].

containing the effects of CM confinement, which will be used in what follows.

4. $V_1(r,T)$ AND THE POLYAKOV LINES

In this section, we analyze Polyakov lines (PL) $L_i, i = \text{adj}, f$, and the np interaction $V_1^{np}(r,T)$, which generates those as functions of temperature. It is fundamentally important, that $V_1^{np}(r,T)$ has a finite nonzero limit at large r, as is seen in (11), and it is exactly this value that enters in L_i at not large n,

$$L_i^{(n)} \simeq \exp\left(-c_i n \frac{V_1^{np}(\infty,T)}{2T}\right),\quad c_{\text{adj}} = \frac{9}{4},\quad c_f = 1. \tag{20}$$

On the lattice PL can be measured in two ways, from the correlator of two PL at the distance r, which yields the singlet free energy $F^s_{Q\bar{Q}}(r,T)$ [25], which is equivalent to $V_1(r,T)$, and includes also the perturbative contributions.

On the other hand, $F_q(T)$ can be found together with L_f from the direct measurement of the fundamental line

$$L^{\text{bare}} = \frac{1}{3}\left\langle Tr\prod_{x_0=0}^{N_c-1} U_0(\mathbf{x}, x_0)\right\rangle_{\text{vac},\mathbf{x}}. \tag{21}$$

The resulting values of the renormalized L are strongly dependent on the type of lattice quark operator used.

In what follows we shall take our L_f using our V_1^{np} from [21], which are in agreement with data from [26].

More explicitly, we are writing for V_1 as in [17]

$$V_1^{np}(\infty,T) = \frac{0.175\text{ GeV}}{1.35\frac{T}{T_0} - 1}. \tag{22}$$

We shall be using these values of V_1^{np} and the corresponding values of $L_i(T)$, Eq. (20), in our Eqs. (15), (16), where S_3 and G_3 are given in (18) to obtain $p(T), I(T)$ and compare to Lattice data.

5. RESULTS AND DISCUSSION

In this section, we present our results for $p(T)$ and $I(T)$ in the temperature region $150\text{ MeV} \le T \le 1000\text{ MeV}$. For $p(T) = \sum_{m_q} P_q^{(m_q)}(T) + P_g(T)$, we are using Eqs. (15), (16) with $G_3(s), S_3(s)$ from (18) and M_f, M_{adj} from (19). The Polyakov lines are obtained from (20), (22). We are using $m_q = 3, 5$, and 100 MeV for $m_q = m_u, m_d$, and m_s, respectively.

We compare in Fig. 1 our results for $\frac{p(T)}{T^4}$ with the lattice results from Table 3 (right column) of [11]. In the following Fig. 2 we report our results for $\frac{I(T)}{T^4}$ in comparison with lattice data from [11] and from [27].

One can see in both Figs. 1 and 2 a good agreement of our results with lattice data. Comparing this with our $p(T)$ from [17], where the same V_1^{np} and Polyakov loops were exploited, but CM confinement in S_3, G_3 was absent, one can deduce, that the CM contribution is very important in the whole interval of T up to

1 GeV. The same is true also for the pure $SU(3)$ theory, studied in [19, 20]. Moreover, in [18] it was shown, that CM confinement solves the old Linde problems, preventing the accurate perturbative calculations in the region $T < 600$ MeV.

Our results show that the FC method can be successfully applied to the quark–gluon thermodynamics and, in particular, it is planned to extend our analysis to the case of nonzero chemical potential.

We specifically excluded from our analysis the region $T < T_0 = 175$ MeV, where the correlator $D^E(x)$ is acting, since the interesting mechanisms of deconfinement and mutual replacements of V_D and V_1^{np} in this region, discussed in [20], require more space and planned for the future.

We are grateful to B.O. Kerbikov and M.A. Andreichikov for useful discussions. This work was supported by the Russian Science Foundation (project no. 16-12-10414).

REFERENCES

1. J. C. Collins and M. J. Perry, Phys. Rev. Lett. **34**, 1353 (1975).
2. N. Cabibbo and G. Parisi, Phys. Lett. B **59**, 67 (1975).
3. E. V. Shuryak, Sov. Phys. JETP **47**, 212 (1978).
4. M. Creutz, Phys. Rev. D **21**, 2308 (1980).
5. L. D. McLerran and B. Svetitsky, Phys. Lett. B **98**, 195 (1981).
6. J. Kuti, J. Polonyi, and K. Szlachanyi, Phys. Lett. B **98**, 199 (1981).
7. P. Braun-Munzinger, V. Koch, Th. Schäfer, and J. Stachel, arXiv:1510.00442 [nucl-th].
8. J. Fingberg, U. M. Heller, and F. Karsch, Nucl. Phys. B **392**, 493 (1993); arXiv:hep-lat/9208012; G. Boyd, J. Engels, F. Karsch, E. Laermann, C. Legeland, M. Lütgemeier, and B. Peterson, Phys. Rev. Lett. **75**, 4169 (1995); arXiv:hep-lat/9506025; Nucl. Phys. B **469**, 419 (1996); arXiv:hep-lat/9602007; B. Beinlich, F. Karsch, E. Laermann, A. Peikert, Eur. Phys. J. C **6**, 133 (1999) [arXiv:hep-lat/9707023.
9. A. Bazavov, N. Brambilla, H.-T. Ding, P. Petreczky, H.-P. Schadler, A. Vairo, and J. H. Weber, Phys. Rev. D **93**, 114502 (2016); arXiv:1603.06637 [hep-lat].
10. A. Bazavov, T. Bhattacharya, G. de Tar et al. (HotQCD Collab.), Phys. Rev. D **90**, 094503 (2014); arXiv:1407.6387 [hep-lat].
11. Sz. Borsanyi, G. Endrödi, Z. Fodor, A. Jakovac, S. D. Katz, S. Krieg, C. Ratti, and K. K. Szabo, J. High Energy Phys. **1011**, 077 (2010); arXiv:1007.2580 [hep-lat].
12. E. Braaten and R. D. Pisarski, Phys. Rev. Lett. **64**, 1338 (1990), J. O. Andersen, E. Braaten, and M. Strickland, Phys. Rev. Lett. **83**, 2139 (1999); arXiv:hep-ph/9902327; J. O. Andersen, M. Strickland, and N. Su, Phys. Rev. Lett. **104**, 122003 (2010); arXiv:0911.0676[hep-ph]; J. O. Andersen, M. Strickland, and N. Su, J. High Energy Phys. **08**, 113 (2010); arXiv:1005.1603 [hep-ph].
13. H. G. Dosch, Phys. Lett. B **190**, 177 (1987); H. G. Dosch, and Yu. A. Simonov, Phys. Lett. B **205**, 339 (1988); Yu. A. Simonov, Nucl. Phys. B **307**, 512 (1988).
14. A. di Giacomo, H. G. Dosch, V. I. Shevchenko, and Yu. A. Simonov, Phys. Rep. **372**, 319 (2002); arXiv:hep-ph/0007223; Yu. A. Simonov, Phys. Usp. **39**, 313 (1996); arXiv:hep-ph/9709344; D. S. Kuzmenko, V. I. Shevchenko, and Yu. A. Simonov, Phys. Usp. **174**, 3 (2004); arXiv:hep-ph/0310190.
15. Yu. A. Simonov, JETP Lett. **54**, 249 (1991), JETP Lett. **55**, 627 (1992); Yu. A. Simonov, Phys. At. Nucl. **58**, 309 (1995); arXiv:hep-ph/9311216.
16. Yu. A. Simonov, in *Varenna-1995: Selected Topics in Nonperturbative QCD, Proceedings of International School of Physics Enrico Fermi, Villa Monastero, June 27–July 7, 1995,* Ed. by A. di Giacomo (IOS Press, 1996), p. 319; arXiv:hep-ph/9509404.
17. Yu. A. Simonov, Ann. Phys. **323**, 783 (2008), arXiv:hep-ph/0702266, E. V. Komarov and Yu. A. Simonov, Ann. Phys. **323**, 1230 (2008); arXiv:0707.0781 [hep-ph].
18. Yu. A. Simonov, arXiv:1605.07060 [hep-ph].
19. N. O. Agasian, M. S. Lukashov, and Yu. A. Simonov, Mod. Phys. Lett. A **31**, 1650222 (2016); arXiv:1610.01472 [hep-lat].
20. N. O. Agasian, M. S. Lukashov, and Yu. A. Simonov, Eur. Phys. J. A (in press), arXiv:1701.07959 [hep-ph].
21. Yu. A. Simonov, Phys. Lett. B **619**, 293 (2005); arXiv:hep-ph/0502078.
22. Yu. A. Simonov, Phys. At. Nucl. **69**, 528 (2006); arXiv:hep-ph/0501182; Yu. A. Simonov and V. I. Shevchenko, Adv. High Energy Phys. **2009**, 873051 (2009); arXiv:0902.1405 [hep-ph]; Yu. A. Simonov, Proc. Steklov Inst. Math. **272**, 234 (2011); arXiv:1003.3608 [hep-ph].
23. N. O. Agasian and Yu. A. Simonov, Phys. Lett. B **639**, 82 (2006); arXiv:hep-ph/0604004.
24. O. Kaczmarek and F. Zantow, Phys. Rev. D **71**, 114510 (2005); arXiv:hep-lat/0503017.
25. L. McLerran and B. Svetitsky, Phys. Rev. D **24**, 450 (1981).
26. O. Kaczmarek, F. Karsch, P. Petreczky, and F. Zantow, Phys. Lett. B **543**, 41 (2002); arXiv:hep-lat/0207002, arXiv:hep-lat/0309121.
27. M. Cheng, S. Ejiri, P. Hegde, F. Karsch, O. Kaczmarek, E. Laermann, R. D. Mawhinney, C. Miao, S. Mukherjee, P. Petreczky, C. Schmidt, and W. Soeldner, Phys. Rev. D **81**, 054504 (2010), arXiv:0911.2215 [hep-lat].